The response of Opalinus Clay when exposed to cyclic relative humidity variations

Katrin M. Wild[1], Patric Walter[1], Florian Amann[1]

[1]Department of Earth Sciences, Geological Institute, ETH Zurich, 8092 Zurich, Switzerland

5 *Correspondence to*: Florian Amann (florian.amann@erdw.ethz.ch)

Abstract. Clay shale specimens were exposed to cyclic relative humidity variations to investigate the response of the material to natural environmental changes. Opalinus Clay, a clay shale chosen as host rock for nuclear waste disposal in Switzerland, was utilized. The specimens were exposed to stepwise relative humidity cycles where they were alternately allowed to equilibrate at 66 and 93% relative humidity. Principal strains were monitored throughout the experiments using strain gauges.

10 After each relative humidity cycle, Brazilian tensile strength tests were performed to identify possible changes in tensile strength due to environmental degradation.

Results showed that Opalinus Clay follows a cyclic swelling-shrinkage behaviour with irreversible expansion limited to the direction normal to bedding, suggesting that internal damage is restricted along the bedding planes. The Brazilian tensile strength in direction parallel and normal to bedding as well as the water retention characteristic remained unaffected by the

15 RH variations.

1 Introduction

In Switzerland, Opalinus Clay, a Mesozoic shale formation of about 180 My years in age, has been selected as the host rock for the disposal of high level nuclear waste (BFE, 2011). Opalinus Clay features several benefitting properties such as its low permeability, the high radionuclide retention, and the potential for self-sealing. However, the favourable characteristics of the

20 rock mass may change during tunnel excavation. Excavation is accompanied by stress redistribution and the development of an excavation damage zone (EDZ). The evolution of the EDZ is an important factor for the long-term safety of a nuclear repository as it may significantly influence the permeability and offer pathways for radionuclide transport. Unloading and/or exposure to atmospheric conditions with a low relative humidity (RH) may lead to suction and in case the air-entry value is exceeded to desaturation of rock mass close to the tunnel. These processes can lead to shrinkage and the formation of

25 desiccation cracks (Tsang et al., 2012). During the open-drift stage of a nuclear repository, seasonal atmospheric changes, especially RH variations, may alter the rock mass and influence the long-term crack evolution. Möri et al. (2010) measured crack apertures of Opalinus Clay in the framework of the Cyclic Deformation (CD) experiment at Mont Terri Underground Rock Laboratory (URL) located in the Jura Mountains, Switzerland. They found that the cracks close during summer (i.e. when the RH is high) and open during winter (i.e. when the RH is low). Crack closure and opening are associated with swelling

and shrinkage of Opalinus Clay. Möri et al. (2010) also observed a net closure of the cracks over several seasonal cycles, which indicates an irreversible deformation component that is likely associated with time-dependent processes such as consolidation, creep or slaking. These irreversible deformation components can contribute to both long-term tunnel convergence and self-sealing of the EDZ. The self-sealing effect is the ability of clay shales to close previously developed cracks and therefore

5   reducing their permeability by hydro-mechanical, hydro-chemical, and/or hydro-biochemical processes (Bernier et al., 2007). Among others, the adsorption of water on clay minerals and related volumetric expansion can be associated with this effect. Numerous studies have been conducted to show the influence of drying/wetting cycles on clay or clay shale specimens (e.g. Chu and Mou, 1973; Popescu, 1980; Chen and Ma, 1987; Osipov et al., 1987; Dif and Bluemel, 1991; Day, 1994; Al-Homoud et al. 1995; Basma et al. 1996; Pejon and Zuquette, 2002). In those studies, however, swelling has been performed by allowing

10   the specimens to fully soak in water. Few studies exist where the influence of cycles in RH on the drying/swelling characteristics of clay shales has been investigated (e.g. Grice, 1968; Van Eeckhout, 1976; Olivier, 1979; Farulla et al., 2010; Cardoso et al., 2011; Pineda et al., 2014). Grice (1968) noted that specimens of Utica shale that were immersed in water disintegrated completely after oven drying. Specimens that were exposed to RH fluctuations between 60 and 90% for a period of 9 months, however, showed only minor cracking. Van Eeckhout (1976) equilibrated specimens of Beatrice coalmine shale

15   to various levels of RH to study the mechanisms of reduction in rock strength resulting from variations in RH. During moisture absorption he measured a volumetric expansion in the order of 0.2-1%. The strains were larger in direction normal to bedding and occurred mostly between 48 and 100% RH. Subsequent drying of the specimens to the initial level of RH showed that about 0.25% of the strains were not recoverable. Van Eeckhout (1976) identified these expansion-contraction characteristics and the associated lengthening in internal cracking as possible cause for the lowering in strength he observed due to humidity

20   fluctuations. Similar observations have been made by Olivier (1979) for specimens of a Lower Triassic mudrock. With the help of water retention curves for several wetting/drying cycles between 10 and 99% RH, Cardoso et al (2011) showed that the air entry value of an Upper Jurassic marl decreases with increasing number of cycles. The decrease is accompanied by an increase in void ratio indicating a degradation of the material. Pineda et al. (2014) experimentally investigated the influence of RH cycles on the degradation of Lilla claystone in a long-term RH cycling experiment using ultrasonic wave velocity

25   measurements and Brazilian tensile strength tests. The applied RH cycles caused an irreversible increase in the specimens' volumes as swelling always exceeded the amount of shrinkage. Pineda et al. (2014) found that higher peak-to-peak amplitudes in RH cycles (cycles between 20 and 99% have been compared to cycles between 50 and 99%) lead to larger volumetric swelling. This effect was less pronounced for specimens that were tested under higher confinements. With the help of microstructural analyses, fissuring has been identified as the main cause for irreversible swelling for Lilla claystone.

30   Furthermore, the degradation of the material was manifested in a decrease of tensile strength from 2.9 MPa to 0.2 MPa after four cycles and a decrease in dynamic Young's modulus by more than 50%. For both quantities, the reduction was largest for the first cycle, afterwards a decreasing degradation rate has been observed.

All studies mentioned above showed that cyclic variations in RH can have a significant influence on rock mechanical parameters such as tensile strength and can lead to irreversible volume changes which might contribute to the destabilisation of underground excavations but also favour processes that are considered to control self-sealing.

5 This study aims at contributing to the understanding of the influence of RH variations on the mechanical and hydro-mechanical behaviour of Opalinus Clay. A series of specimens were exposed to RH variations under unstressed conditions and tested for their Brazilian tensile strength. The study focuses on answering the question if Opalinus Clay shows a damage evolution when exposed to RH cycles that affects the tensile strength and causes irreversible volumetric expansion that might be relevant for long-term deformations and/or self-sealing.

2 Tested material and experimental procedure

10 ### 2.1 Material description

For this study, samples from the shaly facies of Opalinus Clay from the Mont Terri URL, Switzerland were used. The formation is part of the Mont Terri anticline that formed during the folding of the Jura Mountains. The present overburden at the URL lies between 230 and 330 m but is estimated to have reached up to 1350 m in the late Tertiary (Thury and Bossart 1999, Mazurek et al. 2006). The shaly facies of Opalinus Clay contains a clay content of 50-80 % (Mazurek, 1998; Klinkenberg et 15 al., 2009; Nagra, 2002; Bossart 2005). The clay minerals can be subdivided into illite (15-25 %), illite/smectite mixed layer phases (10-15 %), kaolinite (20-30 %), and chlorite (5-15 %). Beside the clay minerals, Opalinus Clay consists of quartz (10-20 %), feldspar (0-5 %), carbonates (5-25 %), pyrite (0-3 %), and organic material (0-1%). The clay particles are aligned sub-parallel to each other leading to a distinct macroscopic bedding. As a result, the physical properties of Opalinus Clay show a strong transversely isotropic behaviour. The hydraulic conductivity, for example, varies between 10^{-12} m/s parallel to bedding 20 and 10^{-14} m/s normal to bedding (Marschall et al., 2004). The water loss porosity of the shaly facies is in the order of 15-19 % (Bossart, 2005; Amann et al., 2011; Amann et al., 2012; Wild et al., 2015; Wild, 2016).

2.2 Sampling and specimen preparation

31 specimens were taken from two 67.5 mm diameter bore cores obtained from a 25 m long borehole (BHM-1) that was drilled in Gallery 08 in the shaly facies of Opalinus Clay at the Mont Terri URL (Fig. 1). A triple-tube core barrel with compressed 25 air cooling was used. The bore axis of BHM-1 was oriented parallel to the bedding. The samples were immediately sealed in vacuum-evacuated aluminium foil after core extraction. Core samples were cut under dry conditions to a diameter to length ratio of approximately 2:1. Additionally, a cubic specimen (S4) was cut in such a way as to allow for the measurement of the principal strains (i.e. the strains perpendicular (ε_1) and parallel (ε_2) to the bedding plane orientation, and the strain in the plane of isotropy (ε_3)). The layout of the electronic strain gauges (HBM type: K-LY41-2/120) that were directly glued on the 30 specimen's faces is shown in Fig. 2a. Furthermore, one cylindrical specimen (E19) was used to measure the strain

perpendicular and parallel to bedding (Fig. 2b). The environmental exposure time of the specimens during the installation of the strain gauges was minimized to about 30 minutes.

2.3 Experimental layout

The specimens were exposed in desiccators to an alternating sequence of low and high RH levels under unstressed conditions. The maximum and minimum level of RH chosen for the laboratory experiment (i.e. 66 and 93% respectively) are based on the seasonal variations at the Mont Terri URL between 1997 and 2011 reported by Swisstopo (2014). It was found that the RH follows a cyclic annual variation following a sine curve with maximum humidity values of 93.8% during summer and minimum humidity values of 62.6% during winter. The RH was controlled by using supersaturated salt solutions. Sodium nitrite ($NaNO_2$, RH = 66% at 20°C) and ammonium di-hydrogen phosphate ($NH_4H_2PO_4$, RH = 93% at 20°C) were used. At each level of RH, the specimens were allowed to equilibrate with the environment. Equilibration was achieved when the weight of the specimens (periodically measured) remained constant. Brazilian tensile strength tests were conducted after each cycle when the specimens were equilibrated at 66% RH. In total 4.5 cycles were applied, starting with an equilibration phase at 93% RH to establish the same initial conditions for all specimens. The experimental setup is schematically shown in Fig. 3. For the monitoring of the RH, a Honeywell HIH-4000-001 sensor (accuracy ±3.5 %) was used. Temperature was monitored by a resistance thermometer (Pt100).

2.4 Suction and strain calculations

The water content was determined according to the ISRM suggested methods (ISRM, 1979). From the RH and the temperature that were monitored during the experiment, the total suction can be calculated according to Kelvin's relationship:

$$\Psi = -\frac{RT}{V_{w0}\omega_w}\ln\left(\frac{p}{p_0}\right), \tag{1}$$

where ψ is the suction in Pa, R is the ideal gas constant (i.e. 8.314 J/mol/K), T the absolute temperature in Kelvin, V_{wo} the specific volume of water (i.e. about 0.001 m^3/kg), ω_w the molecular mass of water vapour (i.e. 0.018 kg/mol), p the vapour pressure of water in the system in MPa, and p_0 the vapour pressure of pure water in MPa. The ratio p/p_0 equals the RH.

On the cubic specimen (S4), strains were measured in all three principal directions. Thus, the volumetric strain (ε_v) can be calculated by adding all three principal strains (i.e. $\varepsilon_v = \varepsilon_1 + \varepsilon_2 + \varepsilon_3$). On the cylindrical specimen (E19), the strain parallel (ε_2) and perpendicular (ε_1) to the bedding was recorded. Assuming a transversely isotropic material, the strain parallel to bedding (ε_2) equals the strain in the plane of isotropy (ε_3). Hence, the volumetric strain can be calculated from the sum of the strain perpendicular to bedding and twice the strain parallel to bedding (i.e. $\varepsilon_v = \varepsilon_1 + 2\varepsilon_2$). For all strains, expansion is taken as positive.

2.5 Mechanical testing procedure

Brazilian tensile strength tests were conducted at ETH Zurich utilizing a modified 2000 kN servo-hydraulic rock testing machine (Walter and Bai, Switzerland). The tests were conducted according to the ISRM suggested methods (ISRM, 1978) immediately after removal from the desiccator. Load was applied parallel (A-specimens) or normal to bedding (E-specimens)

5 (Fig. 4) using a constant loading rate between 0.05 and 0.08 kN/s.

3 Results

The specimens' dimensions and initial properties are given in Table 1. The initial water contents of the specimens range between 6.95 and 7.34 %, which is comparable with the water content measured on cores right after core extraction (Pearson et al. 2003, Amann et al. 2011, Wild et al. (submitted)). The initial saturation was estimated from the initial water content, the

10 bulk dry density, and the porosity of the specimens according to the ISRM suggested methods (ISRM 1979). A grain density of 2.73 g/cm^3 was used to calculate the porosity (Pearson et al., 2003; Bossart, 2005; own data). Values of saturation that exceed 100% can be related to the uncertainty in the grain density (± 0.03 g/cm^3) and the specimen's volume.

Fig. 5 shows the results of the RH, temperature and strain measurements for the E-specimens. The specimens were first equilibrated to a RH of 93% and then subjected to 4.5 cycles with peak-peak amplitudes between 30 and 36% (i.e. RH variation

15 between 63% and 94%; Fig. 5a). The temperature was kept between 19 and 23°C throughout the experiment. The resulting suction applied to the specimens was calculated according to Eq. (1) and is plotted together with the corresponding response of the water content in Fig. 5b. Similar trends with respect to the water content changes were observed for all specimens. A constant water content and a small change in volumetric strain were observed during the first equilibration phase indicating a high initial saturation degree of the specimens. During cycling, the water content changed by ±2.2-2.4%. Except for the first

20 drying period where 0.6-0.8% water content was lost, the water content was reversible. A comparable response was observed for the series of A-specimens (Fig. 6) which were subjected to the same testing procedure, although RH or strains were not measured explicitly. Strain measurements on the specimens E19 and S4 showed an immediate response to changes in RH (Fig. 5c, d). Swelling occurred during wetting, shrinkage during drying phases. The magnitude of swelling exceeded the shrinkage, which accumulated to an irreversible volumetric strain of 0.55-0.75% at the end of the experiment (Fig. 5d). The individual

25 strain measurements showed that mainly deformations normal to bedding contributed to the overall expansion of the rock specimen. The strain measured parallel to bedding was significantly smaller and approximately reversible.

Although irreversible strain was measured, no significant change in Brazilian tensile strength was observed (Fig. 7). The Brazilian tensile strength parallel to bedding remained constant over three to five cycles while corresponding values for the direction normal to bedding only indicate insignificant decreasing trends that lie within the strength values reported by Wild

30 et al. (2015) for specimens that were equilibrated to 56-87 MPa suction. Thus, a change in Brazilian tensile strength as a response to the RH variations was not measurable or insignificant.

4 Discussion

4.1 Water retention

Figure 8 shows the relationship between suction and water content for specimen E7 during the stepwise cyclic RH experiment. The system is in equilibrium at the highest and lowest suction values (turning points between wetting and drying paths) but

5 not in between. Also shown are the main drying and wetting paths reported by Wild et al. (2015).

The first drying path for the specimen follows the main drying path as it represents the drying of the intact rock starting from initial conditions which were comparable to the study of Wild et al. (2015). Since the specimens were not dried to their residual water content, the following scanning curves lie between the main drying and main wetting paths. Hysteresis can be observed between drying and wetting path caused by non-homogeneous pore size distribution, different contact angles between wetting

10 and drying, or entrapped air bubbles during wetting (Birle et al., 2008). Therefore, the initial water content cannot be re-established anymore and a water loss of 0.6-0.8% occurred. However, the scanning curves of the specimen subjected to the stepwise RH cycles approximately lie within the main drying and wetting paths, indicating that the water retention characteristics are not significantly affected by the variations in RH. This is consistent with findings by Pineda et al. (2014).

4.2 Strain and damage

15 Strain results of the dynamic and stepwise cyclic RH experiments (Fig. 5c) indicate that the Opalinus Clay follows a cyclic expansion and contraction associated with water absorption and desorption processes. Thereby, the Opalinus Clay shows a strongly transversely isotropic deformation behaviour where the strain in direction normal to bedding (ε_1) dominate the bulk deformation. These results are consistent with findings by Minardi et al. (2016) who also found an anisotropic response of strain for an Opalinus Clay specimen subjected to one cycle of wetting and drying. This observation can be related to the

20 absorption of water into parallel orientated clay interlayers (i.e. parallel to the bedding planes) leading to swelling in normal direction. Moreover, according to Houben et al. (2013), the pores of Opalinus Clay are elongated along the bedding.

Irreversible volumetric expansion took place during the stepwise cyclic RH exposure. Many studies on single mineral types (e.g. Na-montmorillonite) have demonstrated that clay minerals show distinct hydration states when exposed to different levels of RH (e.g. Mering, 1946; Mooney et al., 1952; Gillery, 1959; Emerson, 1962; Van Olphen, 1965; Glaeser and Mering, 1968;

25 Chipera et al., 1997; Ferrage et al., 2005; Likos and Lu, 2006). These hydration stages reflect the intercalation of one to four discrete layers of water molecules between the mineral interfaces and is driven by the hydration of the cations of the clay minerals (Norrish, 1972). During transition between these stages, the interlayer spacing can increase up to a factor of two (Norrish, 1954). For the hydration of Na-montmorillonite, for example, the interlayer spacing increases from 10 to 12.5 Å between 0 and 20% RH, from 12.5 to 15.5 Å between 50 and 70% RH, and further to about 19 Å for RH>98.5% (Mooney et

30 al., 1952; Gillery, 1959; Emerson, 1962; Glaeser and Mering, 1968). Between 70 and 95% a two-layer hydration state is present for both Ca- and Na-montmorillonite (Seedsman, 1985). Similar stages for other clay minerals are given by Gillery (1959).

They all indicate a relative stable state between 80 and 90% RH. Furthermore, sorption and adsorption paths for clay minerals show hysteresis indicating that crystalline swelling is an irreversible thermodynamic process (Laird et al., 1995).

This might explain the accumulated irreversible volumetric expansion as most of the clay minerals transition between the one- and two-layer hydration state in the RH range covered within the experiments in this study. This is also supported by

5 macroscopically detectable fissuring that was observed during the experiment.

Although slight fissuring of the specimens was detected and irreversible volumetric strain was observed, no significant influence on the Brazilian tensile strength was observed after three to five cycles for both experiments. It is therefore concluded, that the observed degradation caused by the cyclic variations of RH in this study is not sufficient to cause severe damage that influences the strength of the material. The lower degradation potential for Opalinus Clay compared to other clay shales when

10 subjected to RH cycling is in agreement with findings reported by Pineda et al. (2011). Compared to Lilla Claystone (Pineda et al., 2008; Pineda et al., 2014), the (tensile) strength and (dynamic) stiffness of Opalinus Clay is significantly less affected by cyclic RH variations.

5 Conclusions

This study demonstrates that cyclic RH variations have the potential to internally damage the Opalinus Clay leading to

15 irreversible volumetric expansion. Internal damage is mainly taking place along the bedding, supported by the fact that irreversible strain was almost exclusively observed in direction normal to the bedding.

The Brazilian tensile strength of Opalinus Clay seems to be unaffected by cyclic RH variations (i.e. a change was not measurable or insignificant). The Brazilian tensile strength parallel to bedding remained constant over three to five cycles while corresponding values for the direction normal to bedding only indicate insignificant decreasing trends. Water retention

20 characteristics of Opalinus Clay were not significantly altered by the observed environmental degradation.

The experimental study demonstrates that environmental variations, in particular long-term variations in RH can lead to irreversible volumetric strains that contribute to long term deformations of underground excavations and favour processes that are considered to control self-sealing in Opalinus Clay.

25 *Data availability.* The data of this study can be provided by the authors upon request.

Author contribution. The experiment was carried out by P. Walter under the supervision of F. Amann and K.M. Wild. K.M. Wild prepared the manuscript with contributions from all co-authors.

30 *Acknowledgements.* This study was funded by the Swiss Federal Nuclear Safety Inspectorate ENSI. The authors would like to thank Reto Seifert and Stewart Bishop (ETH Zurich) for their support with the mechanical and electrical challenges during the setup of the experiment. We are also grateful to Matthew Perras and Wilfried Winkler (ETH Zurich) for the fruitful discussions. Furthermore, we would like to thank Claudio Madonna (ETH Zurich) for help provided during the laboratory work and for reviewing this paper.

References

Al-Homoud, A.S., Basma, A.A., Husein Malkawi, A.I., and Al Bashabsheh, M.A.: Cyclic Swelling Behavior of Clays, J. Geotech. Eng., 121, 562-565, 1995.

5   Amann, F., Button, E.A., Evans, K.F., Gischig, V.S., and Blümel, M.: Experimental study of the brittle behavior of clay shale in rapid unconfined compression, Rock Mech. Rock Eng., 44, 415-430, 2011.

Amann, F., Kaiser, P.K., and Button, E.A.: Experimental study of the brittle behavior of clay shale in rapid triaxial compression, Rock Mech. Rock Eng., 45, 21-33, 2012.

Basma, A.A., Al-Homoud, A.S., Husein Malkawi, A.I., and Al-Bashabsheh, M.A.: Swelling-shrinkage behavior of natural
10   expansive clays, Appl. Clay Sci., 11, 211-227, 1996.

Bernier, F., Li, X.L., Bastiaens, W., Ortiz, L., Van Geet, M., Wouters, L., Fireg, B., Blümling, P., Desrues, J., Viaggiani, G., Coll, C., Chanchole, S., De Greef, V., Hamza, R., Malinsky, L., Vervoort, A., Vanbrabant, Y., Debecker, B., Verstraelen, J., Govaerts, A., Wevers, M., Labiouse, V., Escof-fier, S., Mathier, J.-F. Gastaldo, L., and Bühler, Ch.: Fracture and Self-healing within the excavation Disturbed Zone in Clays (SELFRAC), Final report, European Commission Report, EUR
15   22585, 62 pp., 2007.

BFE (Bundesamt für Energie): Press Release 01.12.2011, Bern, Switzerland, 2011.

Birle, E., Heyer, D., and Vogt, N.: Influence of the initial water content and dry density on the soil-water retention curve and the shrinkage behavior of a compacted clay, Acta Geotech., 3, 191-200, 2008.

Bossart, P.: Characteristics of Opalinus Clay at Mont Terri. Pdf available at http://www.mont-terri.ch/internet/mont-
20   terri/de/home/geology/key_characteristics.html, last visit: 11.7.2016, 2005.

Cardoso, R., Della Vecchia, G., Jommi, C., and Romero, E.: Water retention curve for evolving marl under suction cycles, in: Alonso, E. and Gens, A. (eds): Unsaturated Soils, Proceedings of the 5th International Conference on Unsaturated Soils, 6-8 September 2010, Barcelona, Spain, 2, 1451-1457, 2011.

Chen, F.H. and Ma, G.S.: Swelling and Shrinkage Behavior of Expansive Clays, in: Proceedings of the 6th International
25   Conference on Expansive Soils, 1-4 December 1987, New Delhi, India, 127-129, 1987.

Chipera, S.J., Carey, J.W., and Bish, D.L.: Controlled-humidity XRD analyses: Application to the study of smectite expansion/contraction, Adv. X Ray Anal., 39, 713-722, 1997.

Chu, T.Y. and Mou, C.H.: Volume change characteristics of expansive soils determined by con-trolled suction tests, in: Proceedings of the 3rd International Conference on Expansive Soils, 30 July-1 August, Haifa, Israel, 2, 177-185, 1973.

30   Day, R.W.: Swell-shrink behavior of compacted clay, J. Geotech. Eng., 120, 618-623, 1994.

Dif, A.E. and Bluemel, W.F.: Expansive Soils under Cyclic Drying and Wetting, Geotech. Test. J., 14, 96-102, 1991.

Emerson, W.W.: The swelling of Ca-montmorillonite due to water absorption, 1. Water uptake in the vapour phase, J. Soil Sci., 13, 31-39, 1962.

Farulla, C.A., Ferrari, A., and Romero, E.: Volume change behaviour of a compacted scaly clay during cyclic suction changes, Can. Geotech. J., 47, 688-703, 2010.

5   Ferrage, E., Lanson, B., Sakharov, B.A., and Drits, V.A.: Investigation of smectite hydration properties by modeling experimental X-ray diffraction patterns: Part I. Montmorillonite hydration properties, Am. Mineral., 90, 1358-1374, 2005.

Gillery, F.H.: Adsorption-desorption characteristics of synthetic montmorillonoids in humid atmospheres, Am. Mineral., 44, 806-818, 1959.

Glaeser, R. and Mering, J.: Homogeneous hydration domains of the smectites, Cr. Acad. Sci. D. Nat., 267, 463-466, 1968.

10   Grice, R.H.: The Effect of Temperature-Humidity on the Disintegration of Nonexpandable Shales, Bull. Asso Eng. Geol., 5, 70-77, 1968.

Houben, M.E., Desbois, G., and Urai, J.L.: Pore morphology and distribution in the Shaly facies of Opalinus Clay (Mont Terri, Switzerland) : Insights from representative 2D BIB-SEM investigations on mm to nm scale, Appl. Clay Sci., 71, 82-97, 2013.

15   ISRM: Suggested Methods for Determining Tensile Strength of Rock Materials, Int. J. Rock Mech. Min., 15, 99-103, 1978.

ISRM: Suggested Methods for Determining Water Content, Porosity, Density, Absorption and Related Properties and Swelling and Slake-Durability Index Properties, Int. J. Rock Mech. Min., 16, 141-156, 1979.

Klinkenberg, M., Kaufhold, S., Dohrmann, R., and Siegesmund, S.: Influence of carbonate micro-fabrics on the failure strength of claystones, Eng. Geol., 107, 42-54, 2009.

20   Laird, D.A., Shang, C., and Thompson, M.L.: Hysteresis in Crystalline Swelling of Smectites, J. Colloid Interf. Scic, 171, 240-245, 1995.

Likos, W.J. and Lu, N.: Pore-scale analysis of bulk volume change from crystalline interlayer swelling in Na+- and Ca2+-smectite, Clay Clay Miner., 54, 515-528, 2006.

Marschall P, Croisé, J., Schlickenrieder, L., Boisson, J.-Y., Vogel, P., and Yamamoto, S.: Synthesis of Hydrogeological

25   Investigations at Mont Terri Site (Phase 1 to 5), in: Heitzmann, P. (ed): Mont Terri Project – Hydrogeological Synthesis, Osmotic Flow. Reports of the Federal Office for Water and Geology, Geology Series, 6, 7-92, 2004.

Mazurek, M.: Mineralogical composition of Opalinus Clay at Mont Terri – a laboratory inter-comparison, Unpublished Mont Terri Technical Note TN 98-41, 1998.

Mazurek, M., Hurford, A.J., Leu, W.: Unravelling the multi-stage burial history of the Swiss Molasse Basin: integration of

30   apatite fission track, vitrinite reflectance and biomarker isomerisation analysis, Basin Res., 18, 27-50, 2006.

Mering, J.: On the hydration of montmorillonite, T. Faraday Soc., 42, 205-219, 1946.

Minardi, A., Crisci, E., Ferrari, A., and Laloui, L.: Anisotropic volumetric behaviour of Opalinus Clay shale upon suction variation, Géotechnique Letters, 6, 144-148, 2016.

Mooney, R.W., Keenan, A.G., and Wood, L.A.: Adsorption of Water Vapor by Montmorillonite. II. Effect of Exchangeable Ions and Lattice Swelling as Measured by X-Ray Diffraction, J. Am. Chem. Soc., 74, 1371–1374, 1952.

Möri, A., Bossart, P., Matray, J.-M., Müller, H., and Frank, E.: Mont Terri project, cyclic deformations in the Opalinus Clay, in: ANDRA (ed): Clays in Natural & Engineered Barriers for Radioactive Waste Confinement, 4th International Meeting, 29 March-1 April 2010, Nantes, France, 81-82, 2010.

Nagra: Projekt Opalinuston. Synthese der geowissenschaftlichen Untersuchungsergebnisse, Nagra Technischer Bericht NTB 02-03, 2002.

Norrish, K.: The Swelling of Montmorillonite, T. Faraday Soc., 18, 120-134, 1954.

Norrish, K.: Forces between clay particles, in: Serratosa, J.M. and Sanchez, A. (eds): Proceedings of the International Clay Conference, 23-30 June 1972, Madrid, Spain, 1, 375-383, 1972.

Nussbaum, C., Bossart, P., Amann, F., and Aubourg, C.: Analysis of tectonic structures and excavation induced fractures in Opalinus Clay, Mont Terri underground rock laboratory (Switzerland), Swiss J. Geosci., 104, 187-210, 2011.

Olivier, H.J.: Some aspects of the influence of mineralogy and moisture redistribution on the weathering behavior of mudrocks, in: Proceedings of the 4th ISRM Congress, 2-8 September, Montreux, Switzerland, 467-474, 1979.

Osipov, V.I., Bik, N.G., and Rumjantseva, N.A.: Cyclic Swelling of Clays, Appl. Clay Sci., 2, 363-374, 1987.

Pearson, F.J., Arcos, D., Bath, A., Boisson, J.-Y., Fernández, A.M., Gäbler, H.-E., Gautschi, A., Griffault, L., Hernán, P., and Waber, H. N.: Mont Terri Project – Geochemistry of Water in the Opalinus Clay Formation at the Mont Terri Rock Laboratory, Reports of the Federal Office for Water and Geology (FOWG), 5, 321 pp, 2003.

Pejon, O.J. and Zuquette, L.V.: Analysis of cyclic swelling of mudrocks, Eng. Geol., 67, 97-108, 2002.

Pineda, J.A., Arroyo, M., Romero, E., and Alonso, E.E.: Dynamic tracking of hydraulically induced claystone degradation, in: Burns, S.E., Mayne, P.W., and Santamarina, C.J. (eds): Deformational Characteristics of Geomaterials, Proceedings of the 4th International Symposium on Deformation Characteristics of Geomaterials, 22-24 September 2008, Atlanta, Georgia, USA, 2, 809-816, 2008.

Pineda, J.A., Mitaritonna, G., Romero, E., and Arroyo, M.: Effects of hydraulic cycling on the stiff-ness response of a rigid clay, in: Alonso, E. and Gens, A. (eds): Unsaturated Soils, Proceedings of the 5th International Conference on Unsaturated Soils, 6-8 September 2010, Barcelona, Spain, 2, 1465-1470, 2011.

Pineda, J.A., Alonso, E.E., and Romero, E.: Environmental degradation of claystones. Géotechnique, 64, 64-82, 2014.

Popescu, M.: Behaviour of expansive soils with a crumb structure, in: Snethen, D. (ed): Proceedings of the 4th International Conference on Expansive Soils, 16-18 June 1980, Denver, Colorado 1, 158-171, 1980.

Seedsman, R.: The behavior of clay shales in water, Can. Geotech. J., 23, 18-22, 1985.

Swisstopo (Bundesamt für Landestopographie): Relative humidity data at Mont Terri rock laboratory. Data acquisition Swisstopo, Mont Terri project, 2014.

Thury, M. and Bossart, P.: The Mont Terri rock laboratory, a new international research project in a Mesozoic shale formation, in Switzerland, Eng. Geol., 52, 347-359, 1999.

Tsang, C.F., Barnichon, J.D., Birkholzer, J., Li, X.L., Liu, H.H., and Sillen, X.: Coupled thermo-hydro-mechanical processes in the near field of a high-level radioactive waste repository in clay formations, Int. J. Rock Mech. Min., 49, 31-44, 2012.

Van Eeckhout, E.M.: The Mechanisms of Strength Reduction due to Moisture in Coal Mine Shales, Int. J. Rock Mech. Min., 13, 61-67, 1976.

5   Van Olphen, H.: Thermodynamics of interlayer adsorption of water in clays. I. – Sodium Vermiculite. J. Colloid Sci., 20, 822-837, 1965.

Wild, K.M., Wymann, L.P. Zimmer, S., Thoeny, R., and Amann, F.: Water Retention Characteristics and State-Dependent Mechanical and Petro-Physical Properties of a Clay Shale, Rock Mech. Rock Eng., 48, 427-439, 2015.

Wild, K.M.: Evaluation of the hydro-mechanical properties and behavior of Opalinus Clay. Dissertation, ETH Zurich,
10   Switzerland, 222 pp, 2016.

Table 1: Properties and test configurations of specimens. Water content, dry density, porosity, and initial saturation were determined according to ISRM (1979). Furthermore, the direction of the applied load with respect to bedding during the Brazilian tensile strength tests is indicated.

specimen no.	diameter	thickness	initial water content	bulk dry density	porosity	initial saturation	direction of applied stress
(-)	(mm)	(mm)	(%)	(g/cm³)	(%)	(%)	(-)
A1	67.32	35.35	6.95	2.30	15.85	100.8	parallel
A2	67.20	34.78	7.13	2.28	16.47	98.7	parallel
A3	67.66	34.70	7.33	2.26	17.10	97.0	parallel
A4	67.61	32.33	7.23	2.24	17.96	90.1	parallel
A5	67.64	35.76	7.02	2.27	16.69	95.7	parallel
A6	67.37	35.94	6.97	2.28	16.47	96.5	parallel
A7	67.59	34.49	7.04	2.28	16.49	97.3	parallel
A8	67.44	35.01	7.01	2.30	15.74	102.4	parallel
A9	67.39	35.27	7.34	2.26	17.09	97.2	parallel
A10	67.58	35.50	7.21	2.27	16.80	97.4	parallel
A11	67.52	34.77	7.20	2.28	16.33	100.7	parallel
A12	67.63	35.06	7.16	2.27	16.96	95.7	parallel
A14	67.54	35.16	7.26	2.26	17.29	94.8	parallel
A15	67.51	34.89	7.27	2.27	17.02	96.8	parallel
E1	67.06	36.47	7.23	2.30	15.59	106.9	normal
E2	67.12	34.51	7.24	2.28	16.35	101.1	normal
E3	67.08	35.17	7.25	2.30	15.74	105.9	normal
E4	67.1	35.18	7.14	2.30	15.82	103.7	normal
E6	67.14	34.79	7.21	2.30	15.85	104.5	normal
E7	67.02	35.74	7.13	2.29	15.97	102.4	normal
E8	67.15	35.06	7.07	2.29	16.15	100.2	normal
E9	67.21	35.64	7.12	2.28	16.42	98.9	normal
E10	67.24	35.17	7.10	2.28	16.62	97.3	normal
E11	67.47	35.07	7.23	2.26	17.29	94.4	normal
E12	67.43	34.98	7.15	2.27	16.79	96.8	normal
E13	67.56	36.08	7.19	2.24	18.08	88.9	normal
E14	67.50	36.06	7.16	2.27	16.73	97.2	normal
E15	67.20	35.78	7.15	2.28	16.65	97.7	normal
E16	67.08	34.23	7.06	2.28	16.41	98.1	normal
E17	67.28	35.40	7.04	2.28	16.57	96.7	normal
E18	67.25	35.26	7.05	2.27	16.73	95.8	normal
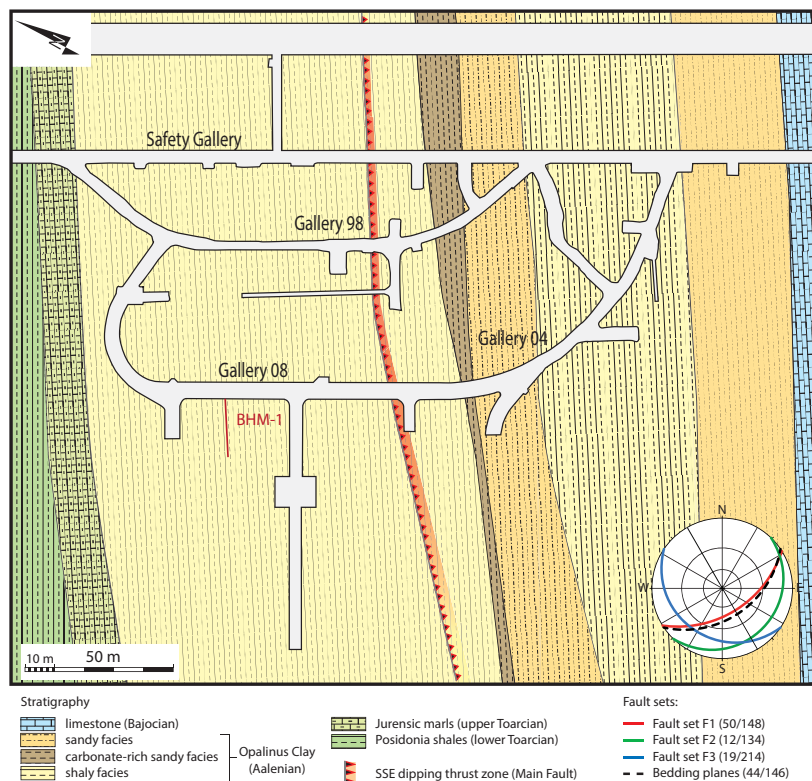
Figure 1: Geological map of the Mont Terri URL (modified from Nussbaum et al., 2011). The specimens used in this study were obtained from the borehole BHM-1 that was drilled parallel to bedding in Gallery 08. The location of the borehole is indicated approximately.
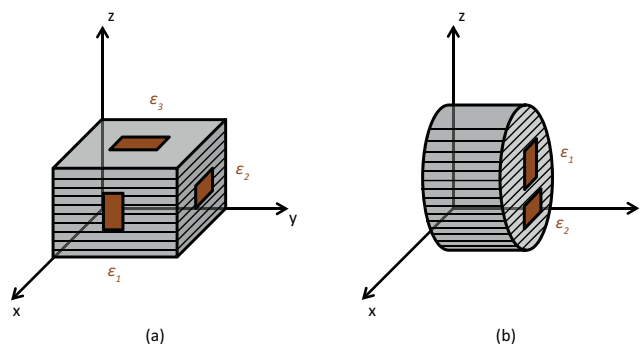
Figure 2: Illustration of strain gauge arrangement for measurements of principal strains: (a) on a cubic Opalinus Clay specimen (S4) measuring all principal strains individually, (b) on a cylindrical Brazilian test specimen (E19) measuring only two principal strains.
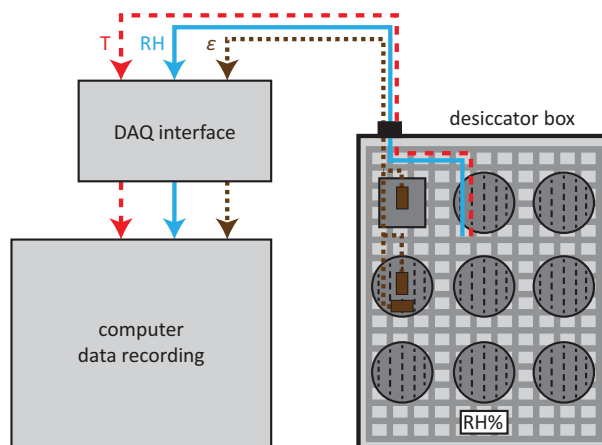
Figure 3: Schematic illustration of the experimental setup of the stepwise cyclic RH laboratory experiment.
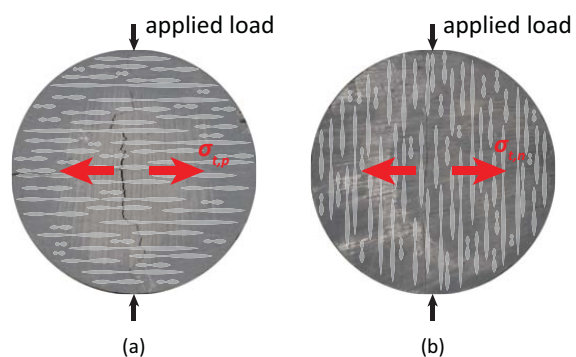
Figure 4: Loading configuration for the Brazilian tests with respect to bedding (bedding orientation is indicated by the light grey pattern). In (a) the load is applied normal to bedding allowing the measurement of the Brazilian ten-sile strength parallel to bedding ($\sigma_{t,p}$). In (b) the load is applied parallel to bedding allowing the measurement of the Brazilian tensile strength normal to bedding ($\sigma_{t,n}$).
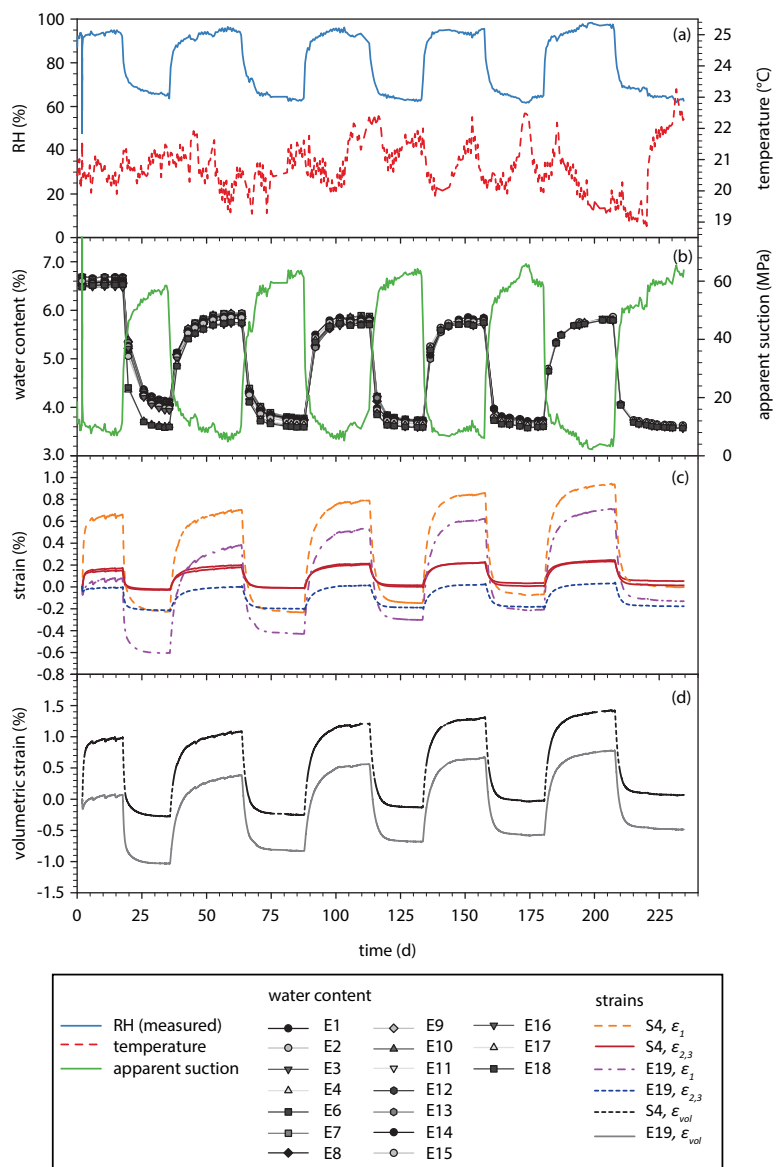
Figure 5: Results of the stepwise cyclic RH experiment for the E-specimens, including (a) the changes in relative humidity (RH) and temperature, (b) the water content and apparent suction calculated from the measured RH, (c) the principal strains normal to bedding (ε_1) and parallel to bedding (ε_2 and ε_3) of specimens S4 and E19, and (d) the volumetric strains of specimens S4 and E19.
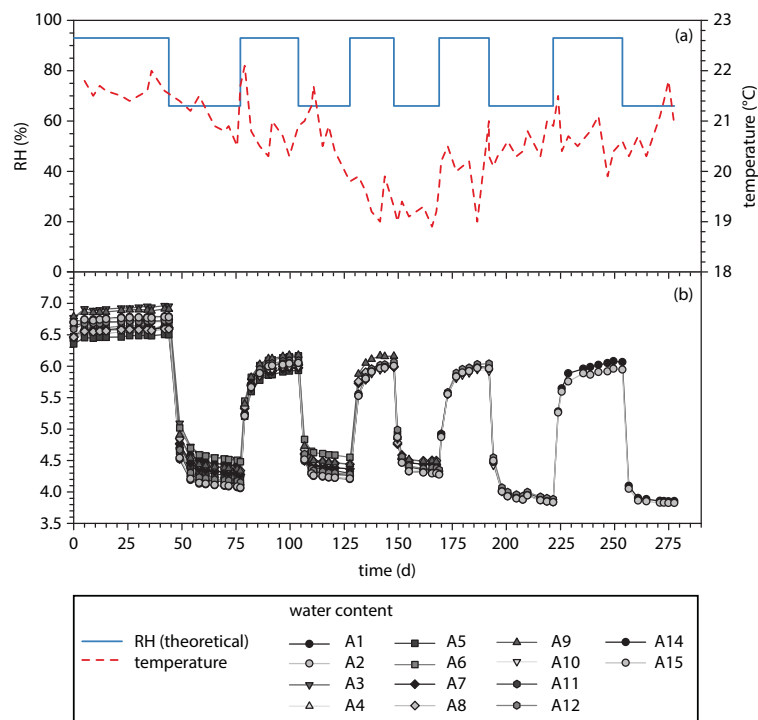
Figure 6: Results of the stepwise cyclic RH experiment for the A-specimens, including (a) the theoretically applied levels of relative humidity (RH) and the measured temperature (in the laboratory), (b) the water content of the specimens.
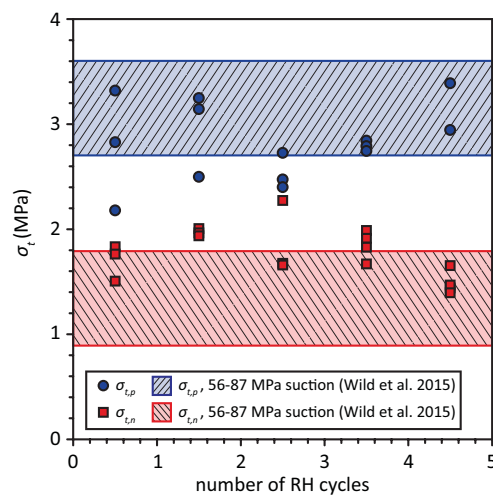
Figure 7: Brazilian tensile strength values of specimens from the stepwise cyclic RH experiment with tension parallel ($\sigma_{t,p}$) and normal ($\sigma_{t,n}$) to bedding. Furthermore, the range of Brazilian tensile strength values reported by Wild et al. (2015) for specimens that were equilibrated to 56-87 MPa suction are indicated.
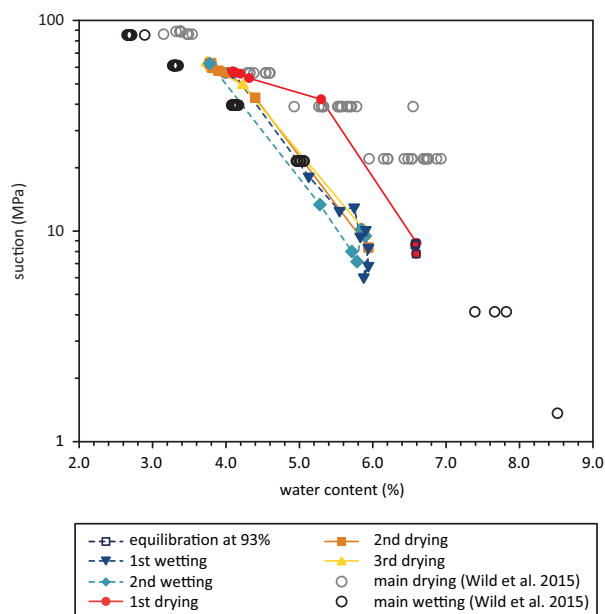
Figure 8: Water retention curve for specimen E7 displaying suction as a function of the water content. Also shown are the water retention curves (main drying and main wetting) reported by Wild et al. (2015) for specimens which were equilibrated to the applied level of RH at any point.